Behav Brain Res. Author manuscript; available in PMC 2018 February 01.

Published in final edited form as:

Behav Brain Res. 2017 February 01; 318: 52–60. doi:10.1016/j.bbr.2016.11.002.

Mapping the dynamics of cortical neuroplasticity of skilled motor learning using micro X-ray fluorescence and histofluorescence imaging of zinc in the rat

Mariam Alaverdashvili[a,b,c,*] and **Phyllis G. Paterson**[a,b]

[a]Neuroscience Research Cluster, Saskatoon, SK, S7N 5E5, Canada

[b]College of Pharmacy and Nutrition, Saskatoon, SK, S7N 5E5, Canada

[c]College of Medicine, University of Saskatchewan, Saskatoon, SK, S7N 5E5, Canada

Abstract

Synchrotron-based X-ray fluorescence imaging (XFI) of zinc (Zn) has been recently implemented to understand the efficiency of various therapeutic interventions targeting post-stroke neuroprotection and neuroplasticity. However, it is uncertain if micro XFI can resolve neuroplasticity-induced changes. Thus, we explored if learning-associated behavioral changes would be accompanied by changes in cortical Zn concentration measured by XFI in healthy adult rats. Proficiency in a skilled reach-to-eat task during early and late stages of motor learning served as a functional measure of neuroplasticity. c-Fos protein and vesicular Zn expression were employed as indirect neuronal measures of brain plasticity. A total Zn map ($20 \times 20 \times 30$ μm^3 resolution) generated by micro XFI failed to reflect increases in either c-Fos or vesicular Zn in the motor cortex contralateral to the trained forelimb or improved proficiency in the skilled reaching task. Remarkably, vesicular Zn increased in the late stage of motor learning along with a concurrent decrease in the number of c-fos-ip neurons relative to the early stage of motor learning. This inverse dynamics of c-fos and vesicular Zn level as the motor skill advances suggest that a qualitatively different neural population, comprised of fewer active but more efficiently connected neurons, supports a skilled action in the late versus early stage of motor learning. The lack of sensitivity of the XFI-generated Zn map to visualize the plasticity-associated changes in vesicular Zn suggests that the Zn level measured by micro XFI should not be used as a surrogate marker of neuroplasticity in response to the acquisition of skilled motor actions. Nanoscopic XFI could be explored in future as a means of imaging these subtle physiological changes.

Keywords

Skilled motor learning; Neural plasticity; Neural efficiency; Synchrotron; Micro X-ray fluorescence imaging; Zinc

*Corresponding author at: Neuroscience Research Cluster, College of Medicine and College of Pharmacy and Nutrition (Mailbox 10), University of Saskatchewan, D Wing Health Sciences 107 Wiggins Road, Saskatoon, SK, S7N 5E5, Canada. mariam.alaverdashvili@usask.ca (M. Alaverdashvili).

1. Introduction

Zinc (Zn) is implicated in regulating neuroplasticity. Zn modulates brain functions, and brain activity modulates Zn level in the brain. Activity-dependent decreases [5] and increases [4,9] in Zn in the barrel cortex of adult mice were observed in response to prolonged sensory (i.e. whisker) stimulation and deprivation, respectively. Exposure of mice to an enriched environment further enhanced the sensory-deprivation induced increase in Zn [37]. Zn also regulates expression of immediate early genes (e.g. c-Fos) in response to brain and behavioral activity through zinc finger transcription factors [18]. Abnormally low amounts of Zn in the brain can also induce learning and memory deficits, although results are not consistent. Whereas administration of Zn chelators affected acquisition and consolidation of hippocampal- and amygdala-dependent memory formation [11,17,27,33,37,46,54], intact spatial learning, memory, and sensorimotor functions have also been reported in mice with depleted vesicular Zn [6].

There is controversy about methodologies used to detect the Zn involved in brain plasticity. Zn can be visualized using various staining techniques. Histochemical [7] and immunofluorescent staining methods [34,39,44] visualize primarily labile Zn. However, these methods also stain other divalent metal cations, including Ca^{+2} [10,38,47], which can overestimate the role of Zn in brain plasticity. A second disadvantage is that the perfusion of a rat as used for most Zn staining procedures can generate artifacts by re-distributing Zn within the tissue [20]. An alternative approach, X-ray fluorescence imaging at the micron level (micro XFI) using a synchrotron generated X-ray source, can provide Zn-specific maps [1,21]. However, since this technique visualizes all zinc, including labile Zn (vesicular and transmembrane intracellular) and Zn bound to proteins participating in chemical catalysis and maintaining protein structure and stability [14,17], this lack of specificity may limit its utility for detecting changes in brain plasticity.

Methodology employing micro XFI has been recently implemented to understand the pathophysiological mechanisms of stroke [3,45,51,55] and the efficiency of various therapeutic interventions that target post-stroke neuroprotection and neuroplasticity, such as hypothermia and physical rehabilitation [3,45]. Although Zn detected by micro XFI has been employed as a plasticity marker after stroke [3,45], it is uncertain if this technique can resolve those Zn alterations due to neuroplasticity. Thus, in the present study, we explored if learning-associated upregulation of c-Fos would be accompanied by changes in Zn concentration measured by two complementary techniques. The *N*-(6-methoxy-8-quinolyl)-*para*-toluenesulfonamide (TSQ) histofluorescence method was used to label vesicular Zn, and synchrotron-based micro XFI was employed to detect all forms of Zn. Proficiency in a skilled reach-to-eat task was employed as the behavioral measure of neuroplasticity. This behavioral paradigm has been widely used to evaluate neuroplasticity both before and after stroke [2,53]. Skilled reaching, the conventional term for the reach-to-eat act, is a form of prehension in which a forelimb is used to reach and grasp a food item and place it into the mouth for eating. Corticospinal pathways in the rat consist of a large crossed pathway, and therefore motor cortex contralateral to the forelimb used for the reach-to-eat act controls and undergoes major plastic changes when a rat is trained for skilled reaching. The structural changes of brain plasticity in neural populations underlying skilled motor action might have

a different temporal profile both in magnitude and direction [22,24,28,35,36] when a skill becomes more automated and efficient. Since skilled motor learning advances through early and late stages of motor learning, a skilled reach-to-eat task is an ideal behavioral paradigm to study neural changes accompanying tuning of neural activity in a particular neural (e.g. Zn rich glutamatergic) population. Therefore, the changes in total and vesicular Zn, and c-Fos were analyzed during the early and late stages of learning of the skilled reaching action. Brain correlates of skilled reaching were studied 15 min after the last training session, since c-Fos protein can be detected within 15–30 min of stimulus application [31].

2. Experimental procedures

2.1. Subjects

Male, Sprague-Dawley (SD) (n = 6) and Long-Evans (LE) rats (n= 10) of comparable age (90–100 days old) were obtained from Charles River (QC, Canada). Rats were housed in Plexiglas cages (36 cm × 20 cm × 21 cm) with absorbent bedding (hardwood and softwood shavings), in groups of two or three in a colony room maintained on a 12 h light/12 h dark cycle (07:00–19:00) with controlled temperature and humidity. This work was approved by the University of Saskatchewan's Animal Research Ethics Board, and adhered to the Canadian Council on Animal Care guidelines for humane animal use.

2.2. Experimental design

Two groups of rats were trained for a skilled reach-to-eat movement [2]. The 20-trial session per day training in a single pellet reaching task (Fig. 1) was for either nine days (early learning stage group; n = 6) or sixteen days (late learning stage group; n = 6). Each of these groups was comprised of 3 LE and 3 SD rats. Each rat was trained to reach with its dominant paw [2] through a narrow slit for a single banana-flavoured sugar pellet (Bio-Serv #F05986) positioned on a shelf outside the reaching box. To be successful, the rat must grasp the food pellet within its paw and bring it to its mouth for eating. The reaching behavior was quantified as the percent of total trials (20 trials) on which a food pellet was successfully obtained. A third group, serving as the control group, was comprised of LE rats (n = 4) exposed for nine days to the same experimental room and the same banana-flavoured sugar pellets; for the latter, control rats were provided the amount of the pellets, that the other rats were successful at eating during training or testing session in the home cages for ~10–15 min on each day. Only four animals were assigned to the control group, because the rats in this group were not subjected to any behavioral manipulation and we expected less variability in measures of brain plasticity. Rats were killed humanely 15 min after the last training session.

Learning-associated neural changes were measured at early and late stages of motor learning. The early stage of learning was defined as the period when success level to retrieve a single pellet was at least 50% for 3 consecutive days of training. The late stage of learning was considered to be the period when the success level was at least 50% for 5–6 days during the second and third week of training.

Learning-associated neural changes were measured only in the caudal area of the forelimb motor cortex, since intensive and massed practice for a skilled reaching action does not induce any significant upregulation of Arc (learning associated immediate early gene) in the trained (vs. nontrained) hemisphere in the rostral area of the forelimb motor cortex [24]. Both layers II/III and V were evaluated for changes in c-Fos and Zn level in the current study because these cortical layers undergo neuroplastic changes as a result of motor skill learning [22,24,28].

2.3. Brain harvesting and sectioning

Animals were anesthetized with 4% isoflurane (1 L/min O_2), and humanely sacrificed through decapitation, with the head immediately flash frozen in liquid nitrogen and stored at −80 °C. The frozen brains were subsequently chiseled out from the frozen heads on dry ice and stored at −80 °C until sectioning [1,21]. Brain tissue was sectioned at a thickness of 30 μm on a cryomicrotome at −16 to −18 °C. These steps in processing of the brain tissue are essential for accurate quantification and localization of Zn. These processing steps preserve *in situ* intracellular Zn distribution and consequently prevent chemical artefacts associated with the Zn diffusion commonly observed when rats are perfused with saline and subsequently fixed with paraformaldehyde solution [21]. Total Zn and c-Fos level were analyzed in all experimental animals. We found sectioning/staining artifact in Zn histofluorescence images in one rat from each of the early and late stage learning groups, and therefore only data from five rats/group were subjected to statistical analysis.

A series of adjacent coronal brain sections were collected from the forelimb and hindlimb regions of the motor cortex at ~0.7 mm anterior to bregma [41] for histochemical, immunohistochemical and XFI analysis. Anatomical references [41] were used to identify the targeted sections. Two of these sections melted onto a sulfur-and metal-free Thermanox plastic coverslip (Thermo Scientific) were subjected to XFI for Zn mapping; subsequent to this, the section was stained with cresyl violet (Nissl substance). The other six sections (at ~0.7 mm anterior to bregma) mounted onto Superfrost slides (VWR) were analyzed for c-Fos immunohistochemistry, cre-syl violet staining, and Zn by histofluorescence. The sections for XFI were air dried and stored in a desiccator in the dark at room temperature prior to analyses; Zn maps were collected within 7 to 10 days of tissue sectioning. The sections for c-Fos immunohistochemistry and Zn histofluorescence were kept at −80 °C until staining.

2.4. c-Fos imaging

2.4.1. Immunohistochemistry—Brain sections were pretreated with 4% paraformaldehyde (PFA) for 5 min and washed three times in 0.01 M phosphate buffered saline (PBS) (pH 7.4). The sections were incubated in 5% Normal Goat Serum (NGS) blocking solution (Sigma, cat# G9023) in 0.01 M PBS at room temperature for 1 h in a Shandon Sequenza immunostaining system. The sections were then incubated with Rabbit polyclonal anti-c-Fos primary antibody (1:1000) (Calbiochem, Cat# PC38) in 0.1% Triton X-100/blocking solution at 4 °C for ~18 h. The sections were rinsed six times in 0.01 M PBS for 5 min each and then immunostained with the goat anti-rabbit secondary antibody tagged with AlexaFluor 594 (1:1000) (Molecular Probes, Invitrogen, cat#A11012) at room

temperature for 2 h. The slides were rinsed six times, 10 min each, in 0.01 M PBS. The sections were coversliped with Prolonged Gold Antifade reagent with DAPI (Invitrogen cat#P36931). To control for variability associated with the immunohistochemical procedures, sections from each experimental group were processed at the same time. As a negative control, the sections (from the caudal area of forelimb motor cortex) from the control and skilled reaching groups were also processed without exposure to the primary antibody; these brain sections showed no labelling.

2.4.2. Image acquisition—The images were acquired using the 20× objective of a BX40 system Olympus microscope and an Evolution VF Monochrome (Media Cybernetics; www.mediacy.com) digital camera using Scope Pro Plus 7 software.

2.4.3. Semiquantitative analysis of c-Fos-immunopositive cells—The c-Fos-immunopositive (c-Fos-ip) cells were counted as the sum from five randomly selected sampling sites of area 322 μm × 240 μm each in layers II/III and layer V in the primary motor cortex within each hemisphere. The c-Fos-ip cells were manually counted from digitized images viewed on a computer monitor with the aid of a computerized image analysis program (NIH Image J v1.62). c-Fos-ip cells were identified by the presence of a red immunoprecipitate on the blue-stained cell nucleus. The immunolabeling ranged from completely red nuclei to nuclei with a speckled appearance. The total number of neurons in each sampling site was determined by counting cells stained with DAPI. The immunoreactivity for c-Fos was quantified as the number of c-Fos-ip neurons/total number of brain cells. The brain regions were identified by cortical cytoarchitecture [56]. Semi-quantitative analysis of c-Fos-ip was conducted by a reviewer blinded to the origin of the sample (behavioral state and trained hemisphere).

For the two trained groups, plasticity-associated changes in c-Fos expression in the trained hemisphere were expressed as relative changes with respect to the untrained hemisphere (Δc-Fos-ip). The latter was calculated as: (number of c-Fos-ip neurons in trained hemisphere/number of total cells in trained hemisphere)/(number of c-Fos-ip neurons in untrained hemisphere/number of total cells in untrained hemisphere) × 100%. To calculate Δc-Fos-ip in the control group, one of the hemispheres was randomly assigned as a pseudo-trained or pseudo-dominant hemisphere. This allowed calculation of Δc-Fos-ip for this hemisphere relative to the pseudo-untrained hemisphere, for comparison against the two trained groups.

2.5. Zinc imaging

2.5.1. X-ray fluorescence method

2.5.1.1. Image acquisition: Zn maps of the motor cortex were collected using micro XFI as previously described [1] at the Stanford Synchrotron Radiation Lightsource (SSRL) experimental station 10-2 (http://www-ssrl.slac.stanford.edu/beamlines/bl10-2/). The energy of the incident X-ray beam was 13 keV. Incident X-ray intensity was measured using a nitrogen gas-filled ion chamber. A monocapillary optic (XOS, East Greenbush, N.Y., USA) was used to generate a microfocused incident beam of approximately 25 μm at the sample when positioned 1 mm away from the optic. The sample was mounted at 45° to the incident

beam and rastered through the beam, with a beam exposure time of 100 ms per 20 μm step. A 4-element Vortex® silicon drift detector at 90° to the incident beam collected the X-ray fluorescence spectra from the brain tissue. The detector readout was synchronised to the stage movement speed, and data was collected continuously, such that the full emission spectrum was collected every 100 ms, for an average stage movement of 20 μm.

2.5.1.2. Quantitative analysis of Zn: X-ray fluorescence imaging data were viewed and analysed using Sam's Microanalysis Toolkit (http://www.sams-xrays.com/#!smak/n44a50) Zn maps were converted from fluorescence intensity to Zn "concentration" (μg/cm^2), using a Zn reference standard, as previously described [1]. Briefly, emission spectra were also collected from a thin film of ZnTe, with a concentration of 45.8 μg/cm^2, on 6 μm of mylar foil (Micromatter, Vancouver). Overlay of Zn images with histological images allowed the cortical layers (the dorsal border of layers I–III and V–VI) to be defined according to cell somata distribution identified by Nissl staining. Regions of interest (ROI) were outlined in layer II/III, layer V, and corpus callosum, and the average amount of Zn within each region was calculated. The Zn concentration of the Thermanox plastic coverslip was also measured, and this background signal was subtracted from the average Zn amount of the brain sample. Zn concentration in each cortical layer was then normalized to the Zn concentration of the corpus callosum from the same section, by expressing the results as a ratio. Normalizing the average Zn amount of each cortical layer reduces data variability caused by any variation in tissue thickness [1] or subtle changes in experimental (i.e. beam) setups at the experimental stations The corpus callosum was used because it contains no glutamergic neurons of high Zn concentration [7] and has a uniform composition such that the main fluctuation in Zn level observed between tissue sections would be expected to come from variation in tissue thickness.

For the two trained groups, plasticity-associated changes in the Zn level of the trained hemisphere were expressed as relative changes (ΔZn) with respect to the untrained hemisphere (%). As described above, ΔZn in the control group was calculated by randomly assigning one of the hemispheres as a pseudo-trained hemisphere.

2.5.2. Histofluorescence method—Vesicular zinc was detected using the *N*-(6-methoxy-8-quinolyl)-*para*-toluenesulfonamide (TSQ) method [15]. Sections were immersed in an aqueous solution of TSQ (4.5 mmol/L) for 60 s, then rinsed for 60 s in 0.9% saline and left to dry. Dried sections were viewed without coverslips.

The aqueous TSQ solution was prepared by dissolving 1.9 g of sodium acetate and 2.9 g of sodium barbital in 100 mL of deionized water, and then adding 0.1 mL of a 1.5% solution (w/v) of TSQ dissolved in hot ethanol [15]. Specifically: (i) 1.9 g of sodium acetate (Sigma Aldrich, Cat# S2889) was dissolved in 41.31 mL of deionized water; (ii) 1 vial of Barbital Buffer (Sigma-Aldrich, Cat#B5934) was reconstituted in 250 mL of deionized water, and 58.69 mL of reconstituted buffer (i.e. 2.9 g of sodium barbital) was added to the sodium acetate solution; (iii) 0.1 mL of a 1.5% solution (w/v) of TSQ (Invitrogen by ThermoFisher Scientific, Cat# M688) was added to the sodium acetate/sodium barbital solution. The solution was made fresh immediately before use and adjusted to pH 10.0.

As a negative control, some of the sections from the control and skilled reaching groups were also processed in sodium acetate/sodium barbital solution without TSQ. The brain sections treated without TSQ yield low fluorescence (~4% of Zn fluorescence observed in experimental samples), and no difference was found between hemispheres. In addition, some of the brain sections containing a hippocampal region, which is rich in histochemically reactive Zn in axon boutons [15], served as positive controls to validate both the staining in our brain samples and efficacy of the TSQ assay.

2.5.2.1. Image acquisition: The TSQ–zinc binding was viewed and the images were acquired using the 10× objective of a BX40 system Olympus microscope and photographed using a fluorescence microscope with 360 nm of ultraviolet light and a 500-nm long-pass filter [48]. The grey scaled images were acquired by Evolution VF Monochrome (Media Cybernetics; www.mediacy.com) digital camera using Scope Pro Plus 7 software.

2.5.2.2. Semi-quantitative analysis of Zn: The Zn signal was measured from digitized images viewed on a computer monitor with the aid of a computerized image analysis program (NIH Image J v1.62). Zn fluorescence intensity within cortical regions was measured as the sum of intensity from two randomly selected sampling sites of area 650 μm × 485 μm each in layers II/III and layer V in the primary motor cortex within each hemisphere. Fluorescence intensity was also measured in corpus callosum, and Zn concentration in each cortical layer was then normalized to the Zn concentration of the corpus callosum from the same section, by expressing the results as a ratio. Since there was no difference in fluorescence signal between hemispheres in the control group, experimental samples were not normalized relative to background Zn level.

For the two trained groups, plasticity-associated changes in the Zn level of the trained hemisphere were expressed as relative changes (ΔZn) with respect to the untrained hemisphere (%). As described above, ΔZn in the control group was calculated by randomly assigning one of the hemispheres as a pseudo-trained hemisphere.

2.6. Cresyl violet staining

Sections were fixed prior to cresyl violet staining using a 4% paraformaldehyde vapor fixation method. Thereafter, the slides were cooled and stained for Nissl substance [1].

2.7. Statistical analysis

Statistical analysis was performed using SPSS 13. Since upregulation of c-Fos expression was considered a positive control for a plasticity-associated change, Δc-Fos-ip data analyses preceded the analyses of the behavioral and ΔZn data. The Shapiro-Wilk test was used to assess the normality of the Δc-Fos-ip data. A two-tailed Student's *t*-test [52] was used to determine if there was any difference in Δc-Fos-ip expression in the primary motor cortex between LE and SD rats both at early and late learning stages. Since there were no differences, the data from the two strains were pooled.

Repeated Measures Analysis of Variance (RANOVA), with Days as the within-subjects variable, was used to assess the effect of training on acquisition of the motor skill in the

single pellet reaching task. When the assumption of sphericity was violated, the degrees of freedom were corrected using the Greenhouse-Geisser estimate of sphericity. *Post hoc* pairwise comparisons with the Bonferroni correction were used to evaluate the difference in success level among the training days.

Δc-Fos-ip and ΔZn in the two groups with early and late stages of motor learning were each compared to the control group using the independent *t*-test. Levene's test for equality of variance was conducted, and if violated, the Welch's *t*-test replaced the Student's *t*-test. In addition, Δc-Fos-ip and ΔZn for the early and late learning stage groups were also evaluated using the One sample *t*-test. Since we did not expect a hemisphere-specific effect in Δc-Fos-ip or ΔZn regardless of whether the control rats were exposed to the environment for 9 or 16 days, our experimental design included only one control group (exposed for 9 days). Nonetheless, the One sample *t*-test was employed as a second analytical approach to overcome this limitation in study design. With this test, Δc-Fos-ip and ΔZn were compared to a preset test value of 100% (i.e. no difference in trained vs. untrained hemisphere). A critical value of 2.015 was obtained for a *t*-distribution (one-tailed) with 5° of freedom (early and late learning stage groups) and a 95% confidence interval [12]. Therefore, *t*-values higher than 2.015 indicated a statistically significant change in Δc-Fos-ip or ΔZn in the two groups of rats exposed to the skilled reach training. A critical value for the t-distribution for vesicular ΔZn of 2.13 was used, since the sample size for this endpoint was only n = 5. The effect size (*r*) was reported for statistically significant changes.

For all analyses, $P < 0.05$ was considered statistically significant. All values are expressed as means ± SEMs.

3. Results

3.1. Effect of rat strain on c-Fos

No rat strain-specific effect for Δc-Fos-ip was observed either at the early (LE: 210 ± 84% and SD: 221 ± 59%; ($t_{\text{Student's}}$ (4) = −0.11, $P > 0.05$) or the late stages of learning (LE: 152 ± 26% and SD: 160 ± 43%); $t_{\text{Student's}}$ (4) = −0.15, $P > 0.05$) in layer V of the motor cortex. Therefore, the rats from both strains were pooled into one group for further analysis.

3.2. Success in a single pellet reaching task

The rats' performance, in a single pellet reaching task, gradually improved with training (the early-stage of learning: (F(2.4, 11.8) = 5.86; $P < 0.01$; $r = 0.8$); the late-stage of learning: (F(11, 55) = 6.39; $P < 0.001$; $r = 0.65$) (Fig. 2). During the first three days of training, the rats mostly explored the reaching cages, used their tongues to get the food pellet(s) placed on the shelf of the reaching cage, or used a paw for reaching for multiple pellets placed directly and adjacent to the slot. The rats started to reach through a narrow slit for a single food pellet on Day 4 of training (i.e. baseline). The success scores reached a statistically significant difference compared to the baseline on Day 7 and thereafter ($P < 0.05$) in both experimental groups.

3.3. c-Fos expression

3.3.1. Early stage of motor learning—The c-Fos-ip cells were observed in layers II/III and V of the motor cortex contralateral to the forelimb trained for 9 days in a skilled reaching action (Fig. 3A). Student's *t*-test yielded higher Δc-Fos-ip in layer V of the motor cortex in the rats exposed to the skilled reaching task compared to the control rats ($t_{\text{Welch's}}$ (5.53) = 2.51; $P < 0.05$; $r = 0.72$) (Fig. 4A). There was no difference in Δc-Fos-ip in layer II/III between the rats with (124 ± 27%) and without training experience (103 ± 4%) ($t_{\text{Welch's}}$ (4.17) = 0.75); $P > 0.05$).

The One sample *t*-test confirmed that Δc-Fos-ip was significantly higher in layer V of the motor cortex ($t_{1\text{-Samp.}}$ (5) = 2.53; $P < 0.05$; $r = 0.75$) but not layer II/III (layer II/III − $t_{1\text{-Samp.}}$ (5) = 2.13; $P > 0.05$) in the rats subjected to skilled reaching training compared to the preset test value.

3.3.2. Late stage of motor learning—Student's *t*-test yielded a trend for higher Δc-Fos-ip in layer V of the motor cortex in the rats subjected to skilled reaching training for 16 days compared to the control rats with no history of training ($t_{\text{Student's}}$ (8) = 2.18; $P = 0.061$; $r = 0.61$) (Fig. 4A). No difference was observed in layer II/III for Δc-Fos-ip between the rats with (347 ± 137%) and without (103 ± 4%) training experience ($t_{\text{Welch's}}$ (5.1) = 1.42; $P > 0.05$).

The One sample *t*-test revealed a significantly higher Δc-Fos-ip in layer V ($t_{1\text{-Samp.}}$ (5) = 2.52, $P < 0.05$; $r = 0.75$) of the motor cortex in the rats subjected to the skilled reaching training compared to the preset test value. Δc-Fos-ip in layer II/III ($t_{1\text{-Samp.}}$ (5) = 1.81, $P > 0.05$) was also not significantly different from the preset test value.

3.4. Total Zn level by micro XFI

3.4.1. Early stage of motor learning—Fig. 3D shows the distribution of total Zn in the motor cortices of a representative rat trained in a single pellet reaching task. Student's *t*-test did not show any difference for total ΔZn in layer V ($t_{\text{Student's}}$ (8) = 0.14; $P > 0.05$) (Fig. 3) or layer II/III (101 ± 6%) ($t_{\text{Welch's}}$ (5.2) = 0.41; $P > 0.05$) of the motor cortex in the rats subjected to skilled motor training compared to the control group (98 ± 6%).

The One sample *t*-test also did not reveal any difference in total ΔZn in layers V ($t_{1\text{-Samp.}}$ (5) = 0.63, $P > 0.05$) or II/III ($t_{1\text{-Samp.}}$ (5) = −0.95, $P > 0.05$) of the motor cortex in the rats with a training history compared to the preset value for the One sample *t*-test.

3.4.2. Late stage of motor learning—There was no difference for total ΔZn in layer V between the rats with and without a training history ($t_{\text{Student's}}$ (8) = −0.65; $P > 0.05$) (Fig. 4B). ΔZn was also comparable in layer II/III between the rats with a high proficiency in skilled reaching (97 ± 3%) and control rats ($t_{\text{Welch's}}$ (5.1) = −0.19; $P > 0.05$).

The One sample *t*-test did not reveal any difference in total ΔZn in layers V ($t_{1\text{-Samp.}}$ (5) = −0.46, $P > 0.05$) or II/III ($t_{1\text{-Samp.}}$ (5) = −1.23, $P > 0.05$) of the motor cortex in the rats subjected to skilled reaching training compared to the preset value.

3.5. Vesicular Zn level by histofluorescence method

3.5.1. Early stage of motor learning—There was no difference in vesicular ΔZn in layer V between the rats with and without a training history ($t_{\text{Student's}}$ (7) = 0.35; $P > 0.05$) (Fig. 4B). ΔZn was also comparable in layer II/III between the rats with a high proficiency in skilled reaching (96± 19%) and control (102 ± 11%) rats ($t_{\text{Student's}}$ (7) = −0.24; $P > 0.05$).

The One sample *t*-test did not reveal any difference in vesicular ΔZn in layers V ($t_{\text{1-Samp.}}$ (4) = 0.42, $P > 0.05$) or II/III ($t_{\text{1-Samp.}}$ (4) = 0.83, $P > 0.05$) of the motor cortex in the rats subjected to skilled reaching training compared to the preset value.

3.5.2. Late stage of motor learning—There was a significant difference for vesicular ΔZn in layer V between the rats with and without a training history ($t_{\text{Student's}}$ (7) = 2.48; $P < 0.05$; $r = 0.68$) (Figs. 3 B and 4 B). However, no difference was observed in layer II/III (111 ± 10%) ($t_{\text{Student's}}$ (6) = 0.67; $P > 0.05$) of the motor cortex in the rats subjected to skilled motor training compared to the control group (102 ± 11%).

The One sample *t*-test also revealed a significant difference in vesicular ΔZn in layers V ($t_{\text{1-Samp.}}$ (4) = 4.26, $P < 0.05$; $r = 0.91$). No difference was found in layer II/III ($t_{\text{1-Samp.}}$ (3) = 0.37; $P > 0.05$) of the motor cortex in the rats with a training history compared to the preset value for the One sample *t*-test.

4. Discussion

Whereas XFI of various trace elements in brain tissue has proven to be a sensitive imaging tool to study the mechanisms of brain injury after stroke, XFI has not yet been validated for elucidating the mechanisms of neuroplasticity associated with spontaneous or therapy-assisted recovery of function following stroke. Since Zn is implicated in neuroplasticity, the present study investigated if cortical Zn level measured by XFI can be used as a surrogate marker of neuroplasticity in the rat.

The single pellet reaching task was chosen as a functional measure of neuroplasticity because learning associated changes have been reported in the motor cortex contralateral to the trained forelimb. Training a rat in a single pellet reaching task increases dendritic branching [19], strength of horizontal connections [42], evoked potential amplitudes [36], and expansion of dendritic spines [23], and causes upregulation of protein synthesis of plasticity- and activity-associated immediate early genes in sensory and motor cortices [22,24]. However, some of these changes may be transient [28,35,36] and specific to only the early stage of motor learning. Dynamic changes in neural activity as skilled reaching becomes more automated might implicate refinning of neural activity in a particular neural (e.g. Zn rich glutamatergic) population. Since the motor skill in a single pellet reaching task advances through early and late stages of motor learning [22,24,28,35,36], we studied changes in Zn and c-fos level after moderate (the early learning stage) and extensive (the late learning stage) training for skilled reaching. To ensure that the training protocol produced plasticity associated changes, the immediate early gene c-Fos was chosen as an established indirect measure of brain plasticity [13,26,30]. Upregulation of c-Fos in the primary motor cortex has been previously linked to learning of motor tasks [24,28].

4.1. Total Zn imaging by micro XFI as a measure of neural plasticity

Zn maps acquired by micro XFI (with 20 × 20 × 30 μm^3 resolution) as used in previous studies to study neuroplasticity following brain ischemia [3,45] failed to detect neuronal changes in rat motor cortex that accompany learning-associated behavioral changes. The improved proficiency demonstrated by an increasing number of successful reaches in the reaching task was not accompanied by a detectable asymmetry in total Zn concentration, quantified by XFI, within the motor cortex in the hemisphere contralateral (vs. ipsilateral) to the trained forelimb. In contrast, increases in the number of c-Fos-ip neurons and vesicular Zn level in the motor cortex contralateral to the trained forelimb paralleled this enhanced proficiency for skilled reaching. The elevated number of c-Fos-ip neurons concomitant with skilled motor learning is in agreement with previous findings [22,24,28], whereas the unaltered total Zn level measured with XFI differs from the findings of the present and previous studies on altered labile Zn in response to brain activity [4,5,9,37].

Several reasons may account for the insensitivity of the XFI-generated Zn map to reveal plasticity-associated changes in the brain: (i) XFI visualizes total Zn, that includes both labile Zn (intra-cellular vesicular and transmembrane Zn) and the Zn bound to proteins that is participating in chemical catalysis and maintaining protein structure and stability [14]. In contrast, only labile, vesicular Zn is visualized by histochemical, histofluorescent [7,15] and immunofluorescent staining methods [34,39,44]. Since the labile Zn pool comprises only ~5% [16] to ~20% of total Zn [7], plasticity associated changes in Zn concentration may be below the detection limits of XFI due to the relatively small change relative to the total Zn level. In our study, the increase in vesicular zinc with late stage motor learning was ~18%. Nevertheless, it is noteworthy that a Zn map generated by XFI was sufficiently sensitive to reveal the previously debated anatomical feature of a cortical layer IV in the motor cortex of the rat; XFI was able to distinguish a “Zn valley” having ~20% less Zn than the adjacent cortical layers II/III and V [1]. (ii) Labile Zn levels in a synaptic cleft are elevated in the nanomolar range in response to closely spaced repetitive neuronal activity [49]. Since skilled reaching is also accompanied by closely spaced repetitive neuronal activity [42] similar to that reported by Vergnano et al. [49] we predicted fluctuations in Zn level due to the skilled reaching action. However, this plasticity-associated change in synaptic Zn is likely below the detection limit of XFI. (iii) Elevated Zn level within the synaptic cleft can be rapid (<30–40 ms) [49] and transient [8,25,49] in order to protect the brain from Zn-induced excitotoxicity [5]. Therefore XFI may not be able to detect plasticity-associated changes in labile Zn associated with fluctuations of synaptic Zn level, since it is impossible to collect brains within the given time frame of “miniature synapatic changes”.

Thus, important methodological evidence has been provided that the Zn level measured by micro XFI should not be considered a surrogate marker of neuroplasticity in response to the training protocol used in our study. Whether Zn maps measured by micro XFI can be useful to visualize plasticity-associated changes in brain regions involved in sensory-motor or cognitive functions with more intensive training protocols or in response to chronic sensory stimulation and deprivation needs further investigation. Nanoscopic XFI [32] which can be used to image single cells, may be able to detect subtle physiological changes occuring in response to the acquisition of skilled motor actions. Furthermore, a multimodal imaging

approach utilizing both XFI and immunohistochemical techniques should be used to distinguish changes in Zn level caused by brain injury from those due to plasticity.

4.2. Brain plasticity at different phases of motor learning

At the late stage of motor learning, a ~1.2 fold increment in vesicular Zn level occurred in parallel with a ~1.6 fold increase of c-Fos-ip neurons in the motor cortex contralateral to the trained forelimb. In contrast, at the early stage of learning, the vesicular Zn level was comparable between hemispheres despite a ~2.2 fold increase in c-Fos-ip neurons in the motor cortex contralateral to the trained forelimb. It is remarkable that vesicular Zn in the trained versus untrained hemisphere increased in the late stage of motor learning. Moreover, this increase was concurrent with a decrease in the number of c-fos-ip neurons compared to that observed at the early stage of motor learning.

Our findings on the timeline of the changes in vesicular Zn level in response to skilled motor learning provide a new insight on plasticity-associated changes in the motor cortex at the late stage of skilled motor learning, although the dynamic of c-fos expression is in agreement with previous findings on structural and functional changes within the motor cortex following skilled motor learning during both the early, acquisition phase [22,24,28,35,36] and the late, maintenance phase [28,36]. A transient expansion of the forelimb representation in the motor cortex (i.e. motor map) [35] specific to the early, acquisition phase of motor learning was previously reported, but it is not clear how neuronal networks change in response to the experience and support the acquired skill. The findings of the present study suggest that as the motor skill advances, there might be a qualitatively different neural population, with fewer active but more efficiently connected neurons, compared to the early stage of the motor learning. The findings also support the idea that glutamatergic and Zn rich neurons i.e. gluzinergic neurons [16] contribute to maintenance of the learned motor skill. This hypothesized pattern of redistribution and/or reorganization of neural activity during different phases of skilled motor learning requires further investigation. The role of vesicular Zn in pre-synaptic plasticity [40] in motor cortex during the late phase of motor learning should be addressed in future studies.

4.3. Layer-specific brain plasticity of skilled motor learning

Training in the skilled reach-to-eat task resulted in a cortical layer-dependent upregulation of c-Fos and vesicular Zn. The number of c-Fos-ip neurons and the level of vesicular Zn significantly increased in layer V after skilled motor learning, whereas c-Fos upregulation was moderate and vesicular Zn was virtually absent in layer II/III. Again, total Zn maps by XFI failed to detect these changes.

A layer specific elevation of the vesicular Zn level in the motor cortex in response to skilled motor learning is the first report of its kind; however layer-specific c-Fos upregulation during the early stage of skilled motor learning was previously reported. Hanlon and colleagues [22] reported that learning associated upregulation of c-Fos stemmed from plasticity changes only in layer II/III of the motor cortex. The discrepancy in layer-specific upregulation of c-Fos in relation to skilled motor learning between the present study and that by Hanlon and colleagues [22] may be explained by differences in allocating anatomical

boundaries for a “deeper” cortical layer (layer V). In the present study, c-Fos-ip neurons were counted only in layer V because of the accumulated knowledge about morphological changes in layer V pyramidal neurons after learning skilled reaching action [29,50]. In contrast, Hanlon and colleagues [22] counted the c-Fos-ip neurons in both layers V and VI, which presumably underestimated plasticity-associated changes in layer V. Additionally, the discrepancy may be related to differences in training procedure.

The plasticity associated increase of c-Fos-ip neurons and vesicular Zn documented in the present study occurred in response to moderate and distributed practice in skilled reaching, whereas previous studies reported learning-associated neuroplastic changes in response to intensive training protocols in the skilled reaching task or prolonged sensory stimulation/deprivation, respectively. In the present study, the rats were subjected to 180 trials in total during nine days of training or 320 trials in total during sixteen days of training, corresponding to the early and late stages of motor learning, respectively. In previous studies, the rats were exposed to 89–150 trials in one day [22,24,36] or 700 trials in total during six days [36]. Since both training protocols promote brain plasticity, either procedure can be employed to improve post-stroke functional recovery. On the one hand, the findings of the present study on c-Fos upregulation during the early stage of motor learning provide further support for the use of a moderate and distributed practice in skilled reaching during the acute and sub-acute post-stroke periods since this approach can prevent fatigue build-up due to intensive and massed practice [43]. On the other hand, if vesicular Zn elevates in the motor cortex only after 320 trials, in the late stage of motor learning, it raises the important question whether prolonged or intensive training would be superior to moderate practice in order to maintain the acquired skill more efficiently. The question is especially critical for future studies on post-stroke rehabilitation procedures in the chronic post-stroke period when stroke survivors tend to forget reacquired skills sooner than healthy counterparts [53]. Nevertheless, removing Zn from synaptic vesicles has been reported to keep intact working and reference memory and gross motor function [6].

5. Conclusions

- A total Zn map generated by micro XFI does not detect cortical neuroplasticity associated with skilled motor learning in the rat.
- The inverse dynamics of c-fos and vesicular Zn level as the motor skill advances through stages suggest that there might be a qualitatively different neural population, with fewer active but more efficiently connected neurons supporting a skilled action in the late compared to the early stage of motor learning.

Acknowledgments

The authors express their gratitude to Drs. Mark J. Hackett, Ingrid J. Pickering and Graham N. George for thoughtful suggestions on analysis of zinc data by XFI. The authors thank Dr. Adil Nazarali for generously providing the microscope for the immunofluorescence study. The authors also thank Angela Cooper for her technical assistance with the immunostaining.

This work was supported by the Canadian Institutes of Health Research (CIHR)/Heart and Stroke Foundation of Canada (HSFC) Synchrotron Medical Imaging Team Grant #CIF 99472 awarded to PGP and others, and a CIHR operating grant (111124) awarded to PGP. M.A. is a Research Associate with the #CIF 99472.

Use of the Stanford Synchrotron Radiation Lightsource (SSRL), SLAC National Accelerator Laboratory, is supported by the U.S. Department of Energy, Office of Science, Office of Basic Energy Sciences under Contract No. DE-AC02-76SF00515. The SSRL Structural Molecular Biology Program is supported by the DOE Office of Biological and Environmental Research, and by the National Institutes of Health, National Institute of General Medical Sciences (including P41GM103393). The contents of this publication are solely the responsibility of the authors and do not necessarily represent the official views of NIGMS or NIH.

References

1. Alaverdashvili M, Hackett MJ, Pickering IJ, Paterson PG. Laminar-specific distribution of zinc: evidence for presence of layer IV in forelimb motor cortex in the rat. Neuroimage. 2014; 103:502–510. [PubMed: 25192655]
2. Alaverdashvili M, Whishaw IQ. A behavioral method for identifying recovery and compensation: hand use in a preclinical stroke model using the single pellet reaching task. Neurosci Biobehav Rev. 2013; 37(5):950–967. [PubMed: 23583614]
3. Auriat AM, Silasi G, Wei Z, Paquette R, Paterson P, Nichol H, Colbourne F. Ferric iron chelation lowers brain iron levels after intracerebral hemorrhage in rats but does not improve outcome. Exp Neurol. 2012; 234(1):136–143. [PubMed: 22226595]
4. Brown CE, Dyck RH. Rapid, experience-dependent changes in levels of synaptic zinc in primary somatosensory cortex of the adult mouse. J Neurosci. 2002; 22(7):2617–2625. [PubMed: 11923427]
5. Brown CE, Dyck RH. Modulation of synaptic zinc in barrel cortex by whisker stimulation. Neuroscience. 2005; 134(2):355–359. [PubMed: 16019150]
6. Cole TB, Martyanova A, Palmiter RD. Removing zinc from synaptic vesicles does not impair spatial learning, memory, or sensorimotor functions in the mouse. Brain Res. 2001; 891(1–2):253–265. [PubMed: 11164830]
7. Cole TB, Wenzel HJ, Kafer KE, Schwartzkroin PA, Palmiter RD. Elimination of zinc from synaptic vesicles in the intact mouse brain by disruption of the ZnT3 gene. Proc Natl Acad Sci U S A. 1999; 96(4):1716–1721. [PubMed: 9990090]
8. Colvin RA, Fontaine CP, Laskowski M, Thomas D. Zn2+ transporters and Zn2+ homeostasis in neurons. Eur J Pharmacol. 2003; 479(1–3):171–185. [PubMed: 14612148]
9. Czupryn A, Skangiel-Kramska J. Differential response of synaptic zinc levels to sensory deprivation in the barrel cortex of young and adult mice. Exp Brain Res. 2001; 141(4):567–572. [PubMed: 11810150]
10. Danscher G, Zimmer J. An improved Timm sulphide silver method for light and electron microscopic localization of heavy metals in biological tissues. Histochemistry. 1978; 55(1):27–40. [PubMed: 76622]
11. Daumas S, Halley H, Lassalle JM. Disruption of hippocampal CA3 network: effects on episodic-like memory processing in C57BL/6J mice. Eur J Neurosci. 2004; 20(2):597–600. [PubMed: 15233771]
12. Field, AP., Hole, GP. How to Design and Report Experiments. Sage Publication Ltd; London: 2003.
13. Filipkowski, RK., Knapska, E., Leszek, K. c-Fos and Zif268 in learning and memory—studies on expression and function. In: Pinaud, R., Tremere, LA., editors. Immediate Early Genes in Sensory Processing, Cognitive Performance and Neurological Disorders. Springer Science + Business Media; New York: 2006. p. 137-158.
14. Frederickson CJ. Neurobiology of zinc and zinc-containing neurons. Int Rev Neurobiol. 1989; 31:145–238. [PubMed: 2689380]
15. Frederickson CJ, Kasarskis EJ, Ringo D, Frederickson RE. A quinoline fluorescence method for visualizing and assaying the histochemically reactive zinc (bouton zinc) in the brain. J Neurosci Methods. 1987; 20(2):91–103. [PubMed: 3600033]
16. Frederickson CJ, Suh SW, Silva D, Frederickson CJ, Thompson RB. Importance of zinc in the central nervous system: the zinc-containing neuron. J Nutr. 2000; 130(5S Suppl):1471S–1483S. [PubMed: 10801962]
17. Frederickson RE, Frederickson CJ, Danscher G. In situ binding of bouton zinc reversibly disrupts performance on a spatial memory task. Behav Brain Res. 1990; 38(1):25–33. [PubMed: 2161241]

18. Gower-Winter SD, Levenson CW. Zinc in the central nervous system: from molecules to behavior. Biofactors. 2012; 38(3):186–193. [PubMed: 22473811]
19. Greenough WT, Larson JR, Withers GS. Effects of unilateral and bilateral training in a reaching task on dendritic branching of neurons in the rat motor-sensory forelimb cortex. Behav Neural Biol. 1985; 44(2):301–314. [PubMed: 2415103]
20. Hackett MJ, McQuillan JA, El-Assaad F, Aitken JB, Levina A, Cohen DD, Siegele R, Carter EA, Grau GE, Hunt NH, Lay PA. Chemical alterations to murine brain tissue induced by formalin fixation: implications for biospectroscopic imaging and mapping studies of disease pathogenesis. Analyst. 2011; 136(14):2941–2952. [PubMed: 21629894]
21. Hackett MJ, Smith SE, Paterson PG, Nichol H, Pickering IJ, George GN. X-ray absorption spectroscopy at the sulfur K-edge: a new tool to investigate the biochemical mechanisms of neurodegeneration. ACS Chem Neurosci. 2012; 3(3):178–185. [PubMed: 22860187]
22. Hanlon EC, Faraguna U, Vyazovskiy VV, Tononi G, Cirelli C. Effects of skilled training on sleep slow wave activity and cortical gene expression in the rat. Sleep. 2009; 32(6):719–729. [PubMed: 19544747]
23. Harms KJ, Rioult-Pedotti MS, Carter DR, Dunaevsky A. Transient spine expansion and learning-induced plasticity in layer 1 primary motor cortex. J Neurosci. 2008; 28(22):5686–5690. [PubMed: 18509029]
24. Hosp JA, Mann S, Wegenast-Braun BM, Calhoun ME, Luft AR. Region and task-specific activation of Arc in primary motor cortex of rats following motor skill learning. Neuroscience. 2013; 250:557–564. [PubMed: 23876329]
25. Howell GA, Welch MG, Frederickson CJ. Stimulation-induced uptake and release of zinc in hippocampal slices. Nature. 1984; 308(5961):736–738. [PubMed: 6717567]
26. Hughes P, Lawlor P, Dragunow M. Basal expression of Fos, Fos-related, Jun, and Krox 24 proteins in rat hippocampus. Brain Res Mol Brain Res. 1992; 13(4):355–357. [PubMed: 1320724]
27. Keller KA, Chu Y, Grider A, Coffield JA. Supplementation with L-histidine during dietary zinc repletion improves short-term memory in zinc-restricted young adult male rats. J Nutr. 2000; 130(6):1633–1640. [PubMed: 10827222]
28. Kleim JA, Lussnig E, Schwarz ER, Comery TA, Greenough WT. Synaptogenesis and Fos expression in the motor cortex of the adult rat after motor skill learning. J Neurosci. 1996; 16(14): 4529–4535. [PubMed: 8699262]
29. Kolb B, Cioe J, Comeau W. Contrasting effects of motor and visual spatial learning tasks on dendritic arborization and spine density in rats. Neurobiol Learn Mem. 2008; 90(2):295–300. [PubMed: 18547826]
30. Kovacs KJ. c-Fos as a transcription factor: a stressful (re)view from a functional map. Neurochem Int. 1998; 33(4):287–297. [PubMed: 9840219]
31. Krukoff, TL. c-Fos expression as a marker of functional activity in the brain. In: Boulton, AA.Baker, GB., Bateson, AN., editors. Cell Neurobiology Techniques, Neuromethods. Humana Press; Totowa: 1999. p. 213-230.
32. Laforce B, Carlier C, Vekemans B, Villanova J, Tucoulou R, Ceelen W, Vincze L. Assessment of ovarian cancer tumors treated with intraperitoneal cisplatin therapy by nanoscopic X-ray fluorescence imaging. Sci Rep. 2016:6. [PubMed: 28442741]
33. Lassalle JM, Bataille T, Halley H. Reversible inactivation of the hippocampal mossy fiber synapses in mice impairs spatial learning, but neither consolidation nor memory retrieval, in the Morris navigation task. Neurobiol Learn Mem. 2000; 73(3):243–257. [PubMed: 10775494]
34. Lee JY, Kim JS, Byun HR, Palmiter RD, Koh JY. Dependence of the histofluorescently reactive zinc pool on zinc transporter-3 in the normal brain. Brain Res. 2011; 1418:12–22. [PubMed: 21911210]
35. Molina-Luna K, Hertler B, Buitrago MM, Luft AR. Motor learning transiently changes cortical somatotopy. Neuroimage. 2008; 40(4):1748–1754. [PubMed: 18329289]
36. Monfils MH, Teskey GC. Skilled-learning-induced potentiation in rat sensorimotor cortex: a transient form of behavioural long-term potentiation. Neuroscience. 2004; 125(2):329–336. [PubMed: 15062976]

37. Nakashima AS, Dyck RH. Zinc and cortical plasticity. Brain Res Rev. 2009; 59(2):347–373. [PubMed: 19026685]
38. Nowakowski AB, Petering DH. Reactions of the fluorescent sensor, Zinquin, with the zinc-proteome: adduct formation and ligand substitution. Inorg Chem. 2011; 50(20):10124–10133. [PubMed: 21905645]
39. Palmiter RD, Cole TB, Quaife CJ, Findley SD. ZnT-3, a putative transporter of zinc into synaptic vesicles. Proc Natl Acad Sci U S A. 1996; 93(25):14934–14939. [PubMed: 8962159]
40. Pan E, Zhang XA, Huang Z, Krezel A, Zhao M, Tinberg CE, Lippard SJ, McNamara JO. Vesicular zinc promotes presynaptic and inhibits postsynaptic long-term potentiation of mossy fiber-CA3 synapse. Neuron. 2011; 71(6):1116–1126. [PubMed: 21943607]
41. Paxinos, G., Watson, C. The Rat Brain in Stereotaxic Coordinates. 6. Academic Press; Burlington: 2004.
42. Rioult-Pedotti MS, Friedman D, Hess G, Donoghue JP. Strengthening of horizontal cortical connections following skill learning. Nat Neurosci. 1998; 1(3):230–234. [PubMed: 10195148]
43. Schmidt, RA., Lee, TD. Human Kinetics Champaign. 1999. Motor Control and Learning: a Behavioral Emphasis.
44. Shen H, Zhang Y, Xu J, Long J, Qin H, Liu F, Guo J. Zinc distribution and expression pattern of ZnT3 in mouse brain. Biol Trace Elem Res. 2007; 119(2):166–174. [PubMed: 17916939]
45. Silasi G, Klahr AC, Hackett MJ, Auriat AM, Nichol H, Colbourne F. Prolonged therapeutic hypothermia does not adversely impact neuroplasticity after global ischemia in rats. J Cereb Blood Flow Metab. 2012; 32(8):1525–1534. [PubMed: 22434072]
46. Sindreu C, Storm DR. Modulation of neuronal signal transduction and memory formation by synaptic zinc. Front Behav Neurosci. 2011; 5:68. [PubMed: 22084630]
47. Stork CJ, Li YV. Intracellular zinc elevation measured with a calcium-specific indicator during ischemia and reperfusion in rat hippocampus: a question on calcium overload. J Neurosci. 2006; 26(41):10430–10437. [PubMed: 17035527]
48. Suh SW, Won SJ, Hamby AM, Yoo BH, Fan Y, Sheline CT, Tamano H, Takeda A, Liu J. Decreased brain zinc availability reduces hippocampal neurogenesis in mice and rats. J Cereb Blood Flow Metab. 2009; 29(9):1579–1588. [PubMed: 19536073]
49. Vergnano AM, Rebola N, Savtchenko LP, Pinheiro PS, Casado M, Kieffer BL, Rusakov DA, Mulle C, Paoletti P. Zinc dynamics and action at excitatory synapses. Neuron. 2014; 82(5):1101–1114. [PubMed: 24908489]
50. Wang L, Conner JM, Rickert J, Tuszynski MH. Structural plasticity within highly specific neuronal populations identifies a unique parcellation of motor learning in the adult brain. Proc Natl Acad Sci U S A. 2011; 108(6):2545–2550. [PubMed: 21257908]
51. Wang X, Qian J, He R, Wei L, Liu N, Zhang Z, Huang Y, Lei H. Delayed changes in T1-weighted signal intensity in a rat model of 15-minute transient focal ischemia studied by magnetic resonance imaging/spectroscopy and synchrotron radiation X-ray fluorescence. Magn Reson Med. 2006; 56(3):474–480. [PubMed: 16894583]
52. Winter CF. Using the Student's *t*-test with extremely small sample sizes. PARE. 2013; 18:1–12.
53. Whishaw IQ, Alaverdashvili M, Kolb B. The problem of relating plasticity and skilled reaching after motor cortex stroke in the rat. Behav Brain Res. 2008; 192(1):124–136. [PubMed: 18282620]
54. Whittle N, Hauschild M, Lubec G, Holmes A, Singewald N. Rescue of impaired fear extinction and normalization of cortico-amygdala circuit dysfunction in a genetic mouse model by dietary zinc restriction. J Neurosci. 2010; 30(41):13586–13596. [PubMed: 20943900]
55. Zheng W, Haacke EM, Webb SM, Nichol H. Imaging of stroke: a comparison between X-ray fluorescence and magnetic resonance imaging methods. Magn Reson Imaging. 2012; 30(10): 1416–1423. [PubMed: 22789844]
56. Zilles K, Zilles B, Schleicher A. A quantitative approach to cytoarchitectonics. VI. The areal pattern of the cortex of the albino rat. Anat Embryol (Berl). 1980; 159(3):335–360. [PubMed: 6970009]

HIGHLIGHTS

- Moderate and distributed practice in skilled reaching promotes neural plasticity.
- c-Fos upregulation parallels the improved proficiency in skilled forelimb use.
- Gluzinergic neurons may contribute to maintenance of the learned motor skills.
- μXFI of cortical Zn doesn’t detect neural plasticity after skilled motor learning.
- Multimodal imaging should be applied to studies on post-stroke brain plasticity.

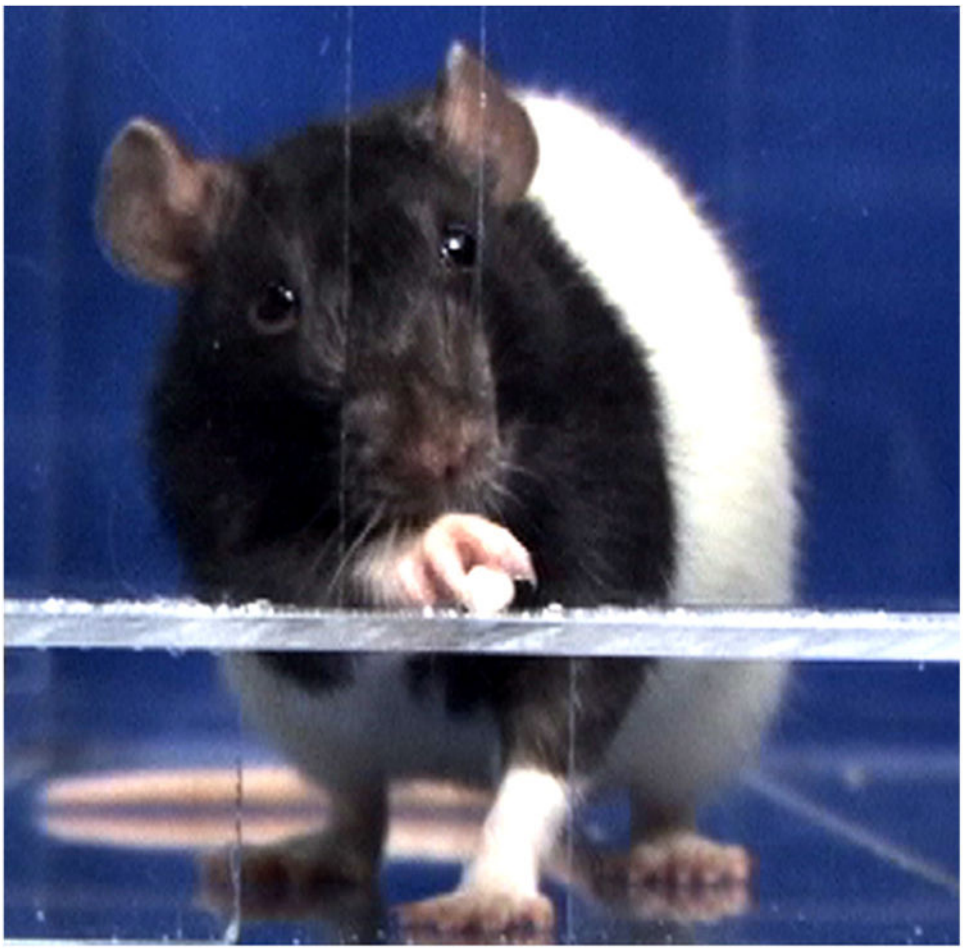

Fig. 1.
A reaching box. A representative rat reaches through a narrow slot for a single pellet.

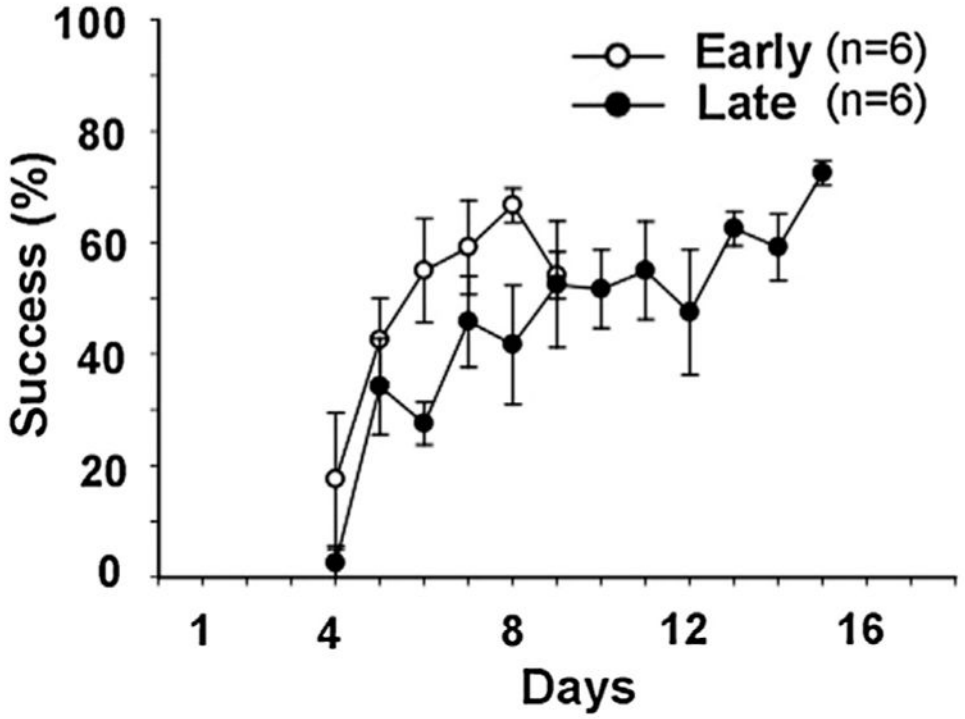

Fig. 2.

Success level in a single pellet reach-to-eat task during early (Early) and late (Late) stages of skilled motor learning (n = 6 for each group); Success (%) = number of successes/20 trials × 100. Day 4 represents the first day on which rats initiated reaching movement by a forelimb for a single pellet. Values are expressed as means ± SEMs.

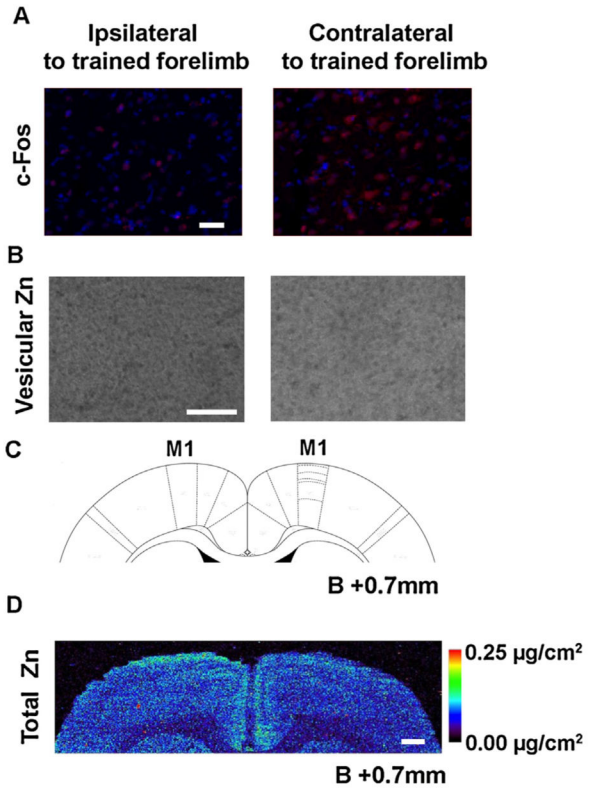

Fig. 3.

c-Fos and zinc (Zn) distribution in the primary motor cortex (M1) at the early stage of skilled motor learning. (A) Representative photomicrographs (20×) of c-Fos staining from layer V of M1: Red—c-Fos; Blue—DAPI. Scale bar = 50 μm. These images were adjusted for contrast (by 40 units) and color balance (red channel by 200% with channel mixture) using Photoshop. (B) Representative grey scaled photographs (10×) of vesicular Zn in layer V of M1 by the histofluorescent *N*-(6-methoxy-8-quinolyl)-*para*-toluenesulfonamide method. Scale bar = 50 μm. (C) Schematic coronal section of a rat brain 0.7 mm anterior from bregma (B + 0.7 mm). The regions drawn with dotted lines (from top to bottom) correspond to the cortical layers I to VI. (C) Total Zn distribution in rat cortical regions at B +0.7 mm measured by synchrotron-based X-ray fluorescence imaging in a representative rat; scale bar = 500 μm. (For interpretation of the references to colour in this figure legend, the reader is referred to the web version of this article.)

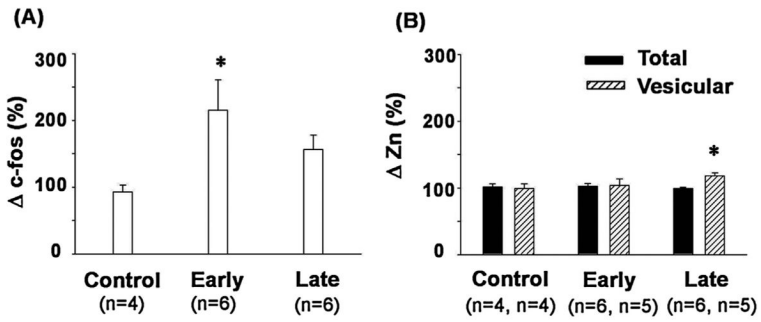

Fig. 4.

The changes in c-Fos (A) and zinc (Zn) concentration (B) in layer V of the primary motor cortex in the hemisphere contralateral to the trained forelimb expressed relative to the ipsilateral hemisphere (Δc-Fos (%) and ΔZn (%), respectively). Early—Early stage of motor learning; Late—Late stage of motor learning. Values are expressed as means ± SEMs. Asterisks indicate significant differences compared to the control group (two-tailed independent *t*-test); $*P < 0.05$. Note the dynamics of learning associated changes in c-Fos expression and vesicular Zn but not in total zinc level measured by synchrotron-based X-ray fluorescence imaging.